

DOI: 10.1002/adma.200800452

# Smooth-Morphology Ultrasensitive Solution-Processed Photodetectors

By Sean Hinds, Larissa Levina, Ethan J. D. Klem, Gerasimos Konstantatos, Vlad Sukhovatkin, and Edward H. Sargent\*

Solution-processed optoelectronic materials offer a route to low-cost photodetectors, large-area solar cells, and integrated optical sources.<sup>[1–3]</sup> While significant progress has been reported in organic and polymer spin-cast optoelectronics, colloidal quantum dots offer a distinct further advantage — the convenient tuning of absorption onset via the quantum size effect.<sup>[4]</sup> Electronic transport has recently been enhanced in size-effect-tuned colloidal quantum dot films using ligand exchange, resulting in ultrasensitive photodetectors in both visible and infrared wavelengths; however, solid-film ligand exchange generally results in rough film morphologies, incompatible with high-uniformity image sensors.<sup>[1,5–7]</sup> The frequent cracking of films is attributed to the significant loss of volume during the exchange process. Here, we report a new route to visible-wavelength spin-cast PbS-nanocrystal photoconductive photodetectors with sub-1% roughness, compared to the ~10% roughness obtained using previously reported approaches. The new procedure yields devices that exhibit  $10 \text{ A W}^{-1}$  responsivities and reveal an added significant advantage: when illumination conditions change, the photodetectors respond with a single time constant of 20 ms. This compares very favorably with the multisecond and multi-time-constant response of previously reported PbS-nanocrystal photoconductive photodetectors.

To be relevant to imaging applications, a top-surface photodetector must exhibit three key traits: high sensitivity to the illumination of interest, spatial uniformity across an imaging array, and video-frame-rate speed of response. *Sensitivity* derives from the photoconductive gain — the number of electrical carriers collected per incident photon given at a specific light level — and the noise-equivalent power (NEP) — the lowest light level that can be distinguished from noise. *Spatial uniformity* better than 1% across a pixel array is sought to minimize the introduction of spatial noise, which produces an image photoresponse nonuniformity of the same order. *Speed of response* allowing video-capture frame rates demands sub-100 ms time constants.

Large photoconductive gains, as high as thousands of electrons collected per incident photon, and large dark resistivities have recently been shown to enable record high

sensitivity in PbS colloidal quantum dot photoconductive photodetectors.<sup>[7]</sup> These devices rely on enhanced charge-carrier mobilities, achieved by chemically displacing their original insulating oleate ligands with shorter ligands. The use of long aliphatic ligands in the synthesis and initial stages of processing prevent aggregation. However, films made from such materials are highly insulating. A procedure to exchange original ligands with shorter ones is needed to achieve sufficiently efficient carrier transport among the nanoparticles. Ligand removal, ligand replacement, and film crosslinking all produce the desired increase in mobility, critical to increased sensitivity; but are accompanied by a significant loss of film volume. This film contraction leads to film cracking — often on multiple length scales ranging from nanometers to micrometers — that renders the resultant film unacceptable for applications demanding exceptional uniformity.<sup>[1,7,8]</sup>

Here, we demonstrate for the first time that useful levels of photoconductive gain and excellent morphology are not mutually exclusive. Solution-phase ligand exchange is the key to this achievement. The challenge we overcome is showing that solution-phase exchange from long to very short ligands can produce a sufficiently stable colloid, and that quantum-size-effect tunability and smooth morphology can be preserved, alongside improved electronic transport.

Our approach was based on the use of short ligands with thiol endgroups. Mercaptan-based ligand exchange has been previously demonstrated to displace oleate ligands on the surface of PbS nanocrystals without compromising size-effect tunability. Reports include thioglycerol, dithioglycerol, and mercapto-undecanoic-11-tetraethyleneglycol.<sup>[9,10]</sup> These reports produced nanoparticles dispersed in water, however, the hydroxides, oxides, and sulfates formed in the aqueous environment generate long-lived trap states on PbS nanoparticles.<sup>[11]</sup>

We therefore sought to produce a stable colloid in a nonpolar organic solvent. For the exchange, we selected short, ethanethiol-terminated ligands, an approach that would have the advantage of enhanced carrier transport in view of the minimal length of its aliphatic chain.

Specifically, we began with oleate-capped PbS nanoparticles dispersed in toluene and having a first excitonic feature at 950 nm. We added an equal volume of ethanethiol, and allowed the mixture to incubate for times ranging from 15 min to multiple hours. We ended the exchange process by precipitating the colloid using hexane. Purely oleate-capped PbS nanoparticles are stable in hexane as well as in toluene. The fact that the addition of hexane precipitated the nanoparticles thus suggests a

[\*] Prof. E. H. Sargent, S. Hinds, L. Levina, E. J. D. Klem, G. Konstantatos, V. Sukhovatkin  
Department of Electrical and Computer Engineering,  
University of Toronto  
Toronto, Ontario, M5S 3G4 (Canada)  
E-mail: ted.sargent@utoronto.ca

significant degree of exchange to the thiol. We centrifuged and resuspended the nanocrystals in chloroform, and fabricated devices by spin-coating the exchanged materials onto planar glass test chips patterned with gold interdigitated electrodes.

Having created a simple process that generates stable solutions of short-ligand-capped nanoparticles, we sought to investigate their impact on film morphology, temporal response, and sensitivity to light.

We used atomic force microscopy (AFM) and profilometry to study the films' surface morphology and thickness. We

investigated i) films made from original (oleic-acid-capped, unexchanged) nanocrystals, ii) films made by spin-casting original nanocrystals, subsequently treated with butylamine, iii) films made by spin-casting nanocrystals previously exchanged to butylamine in the solution-phase, and iv) films made by spin-casting nanocrystals previously exchanged to ethanethiol in the solution-phase.

We present in Figure 1 the impact of these exchange procedures on film morphology. Upon drying, films made from original nanocrystals exhibit large regions of extensive

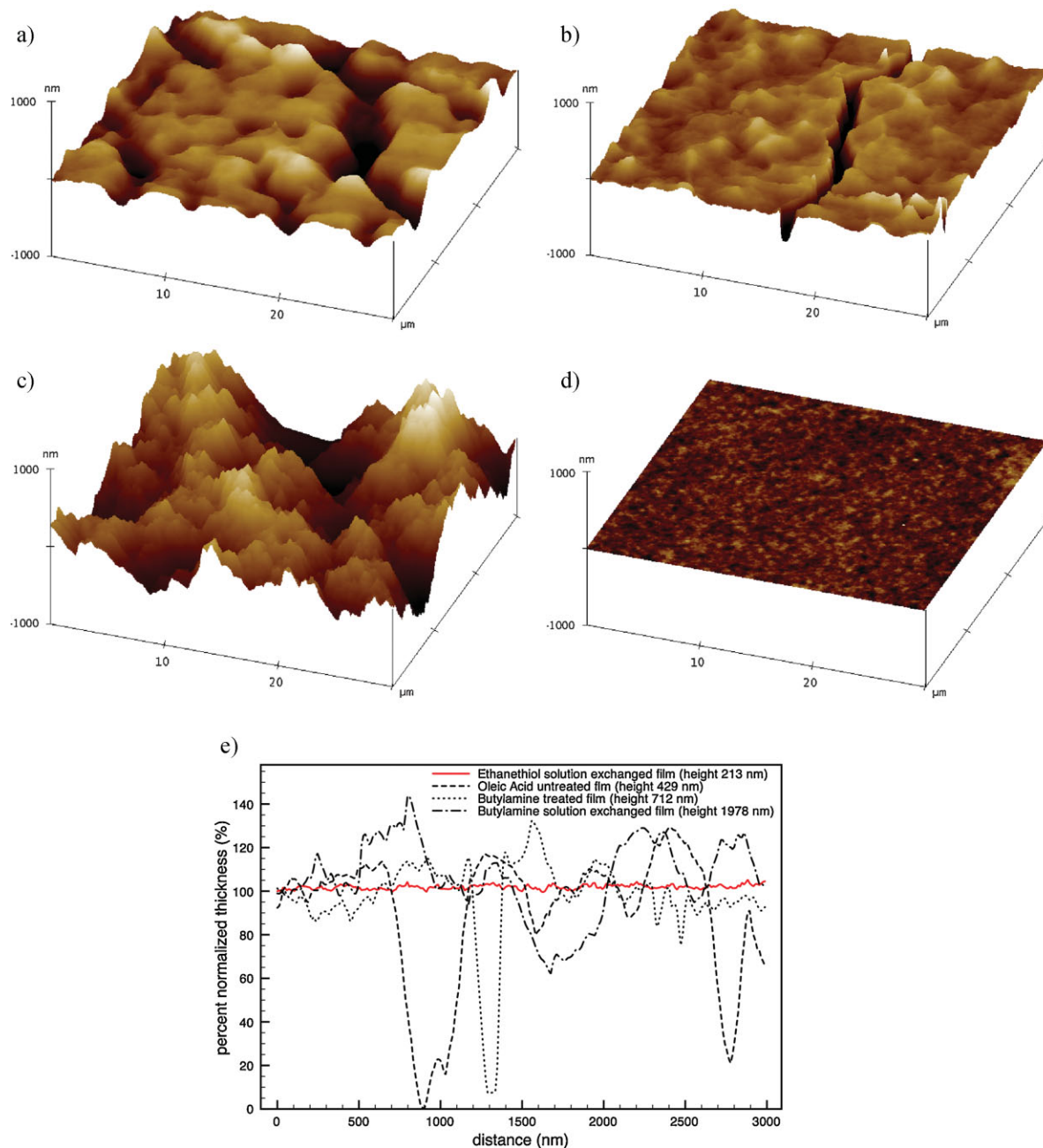


**Figure 1.** a–d) AFM morphology and average roughness of studied PbS nanocrystal films spin-cast on clean glass surfaces. e) Profilometry of normalized height, computed as  $(d - d_0)/d_0 \times 100$  where  $d$  is the thickness of the film, for film thicknesses of a) 429 nm, b) 712 nm, c) 1978 nm, and d) 213 nm.

cracking, with a roughness of 25% of their thickness. When such films were subsequently treated with butylamine, they continued to show cracks but their roughness was somewhat reduced, to 9% of their thickness. Films made from nanoparticles exchanged to butylamine in the solution-phase exhibited 15% roughness. In contrast, films made by spin-coating ethanethiol-solution-exchanged quantum dots yielded crack-free films with 0.7% roughness. The film shown in Figure 1d is slightly over 200 nm thick, and therefore suited to optical-sensor fabrication in view of the substantially complete absorption of visible light in films of this thickness.

We sought to investigate further why solution exchange to butylamine fails to produce films with good morphologies. We compare in Figure 2b–d transmission electron microscopy (TEM) images of as-synthesized, butylamine-solution-exchanged, and ethanethiol-solution-exchanged PbS nanoparticles that absorb visible light. The butylamine-solution-exchanged nanoparticles have aggregated considerably, some of them forming worm-like structures, with clusters of nanoparticles as large as 20–40 nm, and fail to pass through 200 nm pore-sized filters. In contrast, the ethanethiol-solution-

exchanged nanoparticles remain as discrete and monodisperse dots, yield optically flat films, and pass through 200 nm pore-size filters. A comparison of oleate capped with ethanethiol-solution-exchanged nanoparticles reveals a smaller interparticle spacing in the ethanethiol case. Because spin-cast ethanethiol-solution-exchanged films were optically smooth, we were able to use interference features in their absorption spectra to estimate their refractive index. We obtained a value of 2.38, compared to the previously reported value of 1.64 for oleic-acid-capped nanoparticle films.<sup>[12]</sup> This finding is consistent with the considerably closer packing of the ethanethiol-solution-exchanged nanoparticles seen in the TEM images.

We anticipated that the effects of aggregation in butylamine-solution-exchanged particles would be noticeable in their absorption spectrum. A pronounced loss of excitonic structure, and a significant red tail in absorption, is indeed revealed in Figure 2a. In contrast, the spectrum of ethanethiol-capped nanoparticles preserves the sharp feature of the as-synthesized particles.

We now turn to the optoelectronic characterization of the devices. Data were obtained at a bias of 10 V applied between two coplanar Au electrodes separated by a 5  $\mu\text{m}$  wide gap and running parallel over a 3 mm device width. We summarize in Table 1 the dark current, photoconductive gain, time response to optical transients, and the percentage variation in film thickness in each case.

The current–voltage curves (Fig. 3a) of ethanethiol-solution-exchanged devices reveal that the devices are photoconductive photodetectors, have high dark resistivity, and have high sensitivity over a large variation in bias. The devices exhibit a photoconductive gain of 26 at 10 V bias. The difference in temporal response among the different photodetectors is particularly noteworthy. Devices made using butylamine treatments produced multiple temporal component responses, including a significantly slow tail of response on the timescale of seconds.<sup>[1,7]</sup> In contrast, ethanethiol-solution-exchanged devices exhibit a single 20 ms time constant, as shown in detail in Figure 3b. As seen in Figure 3c, the decay time and responsivity of ethanethiol-solution-exchanged devices do not vary greatly as a function of illumination intensity. This observation further suggests the presence of a single-valued trap-state lifetime. Butylamine-treated

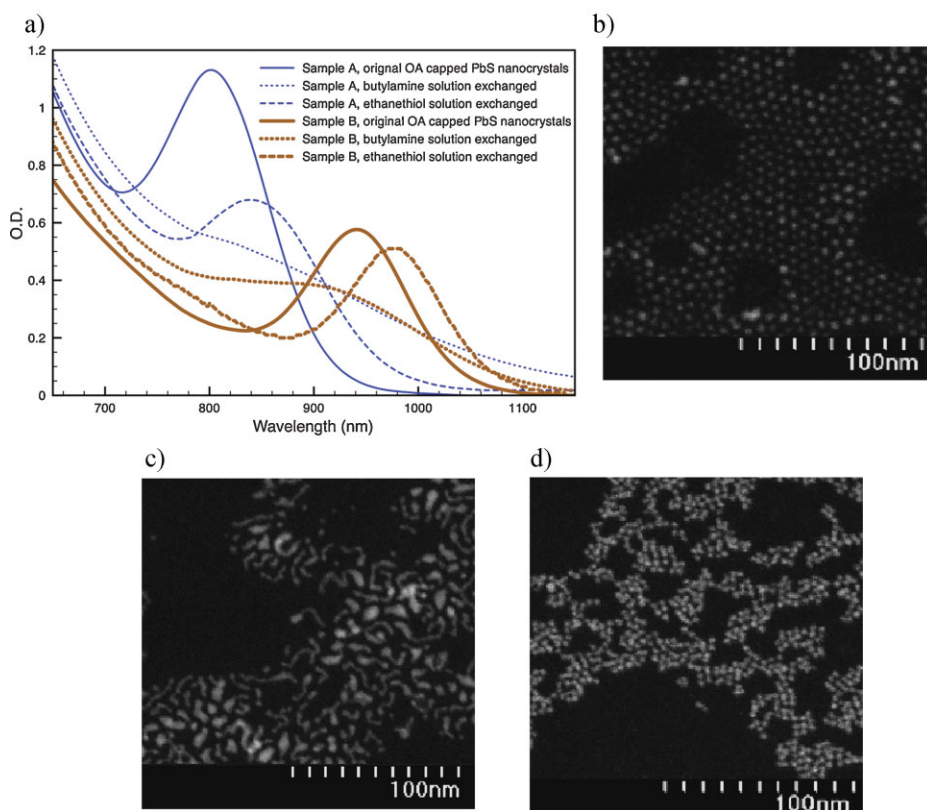


**Figure 2.** a) Absorption spectra of drop-cast PbS nanocrystal films. Samples A and B are from different syntheses. The figure enables the comparison between original (oleic-acid-capped), butylamine-solution-exchanged, and ethanethiol-solution-exchanged films. b–d) Dark field electron microscopy images at 200 kV  $\times$  250 k magnification on formvar-coated 200 mesh copper grids comparing the deposition of typical b) original (unexchanged) nanocrystals, c) butylamine-solution-exchanged nanocrystals, and d) ethanethiol-solution-exchanged nanocrystals.

**Table 1.** Comparison of photoconductive photodetector performance for PbS colloidal quantum dot devices produced using the films in Figure 1 and 2. Percent thickness nonuniformity is defined as roughness average thickness  $\times 100$ . All devices were characterized using  $5 \mu\text{m}$  Au interdigitated gaps biased at 10 V under 470 nm excitation at  $815 \text{ nW cm}^{-2}$ . Note: experimental comparison to butylamine treatments are commensurate with their previously reported performance.<sup>[1,7]</sup>

	Original	Butylamine-treated film	Butylamine-solution exchange	Ethanethiol-solution exchange
Dark current [nA]	0.001	2	116	1.6
Photoresponse time constant [ms]	–	2000	>500	20
Photoconductive gain	–	55	210	26
Average roughness [nm]	100	60	340	1.4
% Thickness nonuniformity	24	9	17	0.7

devices, in contrast, exhibit a significant dependence of temporal response and responsivity on illumination intensity.<sup>[7]</sup>

It was recently shown that the temporal response of PbS colloidal quantum dot photodetectors may be traced to specific chemical species on nanoparticle surfaces.<sup>[11]</sup> Long-tailed transient components are associated with Pb-carboxylates (associated with unremoved oleic acid ligands) and sulfates ( $\text{PbSO}_4$ ). Ethanethiol was found to replace oleic acid and remove sulfates. These and the present work's findings

illustrate that while these photoconductive photodetectors do exploit trap states to achieve gain, it is possible to engineer the combination of transport and trap lifetime to achieve an attractive combination of gain and temporal response. Indeed, the response of the butylamine-treated film provides no advantage in gain over its ethanethiol-exchanged counterpart, in exchange for its highly undesired long-lived temporal response.

In summary, we report ethanethiol-solution-exchanged PbS nanocrystal devices that combine a photoconductive gain of 26,

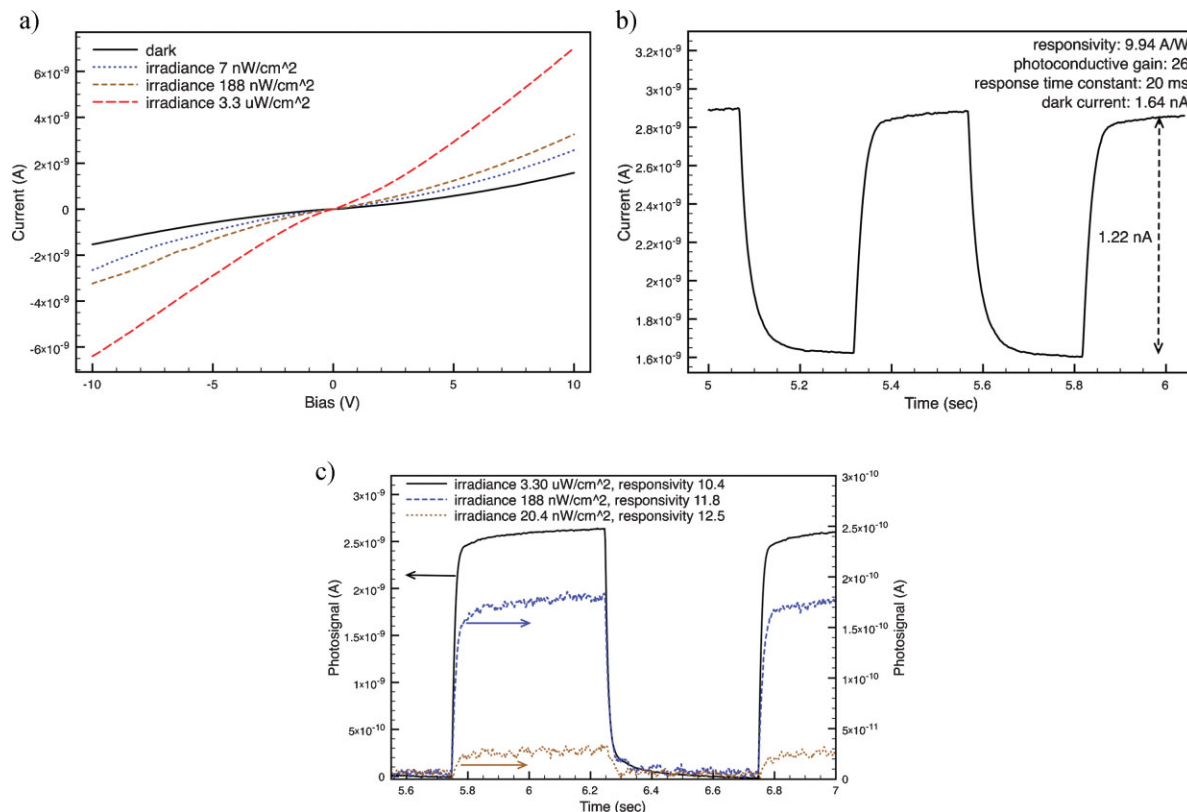


**Figure 3.** Optoelectronic properties of typical ethanethiol-solution-exchanged nanoparticle devices. a)  $I$ - $V$  under dark illumination and under illumination intensities of  $7 \text{ nW cm}^{-2}$ ,  $188 \text{ nW cm}^{-2}$ , and  $3.3 \mu\text{W cm}^{-2}$ . b) Photocurrent temporal response at  $815 \text{ nW cm}^{-2}$  illumination intensity. c) Photosignal as a function of time for illumination intensities of  $20 \text{ nW cm}^{-2}$ ,  $188 \text{ nW cm}^{-2}$ , and  $3.3 \mu\text{W cm}^{-2}$ .

a single time-constant temporal response of 20 ms, and a smooth film morphology with roughness equal to 0.7% of the average thickness.

## Experimental

**Synthesis:** PbO (0.9 g, 4.0 mmol), oleic acid (2.67 g, 9.50 mmol), and octadecene (4.73 g, 18.8 mmol) were mixed (solution A). Hexamethyldisilathiane (210  $\mu$ L) was mixed with octadecene (10 mL) in a nitrogen glove box (solution B). Solution A (19.5 mL) was injected into a flask under argon and the temperature of the solution was raised to 120 °C under heavy stirring. Solution B was then injected into this flask, after which the solution was allowed to cool. When the temperature reached  $\sim$ 35 °C the reaction was quenched with acetone (40 mL). The mixture was then washed repeatedly by suspensions in toluene and precipitations in acetone.

**Film Formation:** Films were formed by spin-coating an ethanethiol-exchanged solution (65  $\mu$ L) of PbS nanocrystals at 700 rpm onto gold interdigitated electrodes on a glass substrate. Absorption spectra were collected using a Cary model 500 spectrophotometer.

Electron microscopy images were acquired using a Hitachi HD-2000 scanning transmission electron microscope at 200 kV.

Responsivity was determined by first subtracting dark current from the light current and then dividing the result by the power striking the active area of the device. The latter was determined as the product of the device area with the uniform intensity generated in a 5 mm diameter collimated 470 nm-wavelength beam. Photoconductive gain is calculated by  $Rhc/(q\lambda)$ , where  $R$  is the responsivity,  $h$  is Planck's constant,  $q$  is the electron charge, and  $\lambda$  is the light wavelength.

Current–voltage characteristics and transient responses were captured using an Agilent 4155 semiconductor parameter analyzer.

Received: February 15, 2008

Revised: May 8, 2008

Published online:

- [1] G. Konstantatos, I. Howard, A. Fischer, S. Hoogland, J. Clifford, E. Klem, L. Levina, E. H. Sargent, *Nature* **2006**, *442*, 180.
- [2] S. A. McDonald, G. Konstantatos, S. Zhang, P. W. Cyr, E. J. D. Klem, L. Levina, E. H. Sargent, *Nat. Mater.* **2005**, *4*, 138.
- [3] Q. Sun, Y. A. Wang, L. S. Li, D. Wang, T. Zhu, J. Xu, C. Yang, Y. Li, *Nat. Photonics* **2007**, *1*, 717.
- [4] N. Cho, K. Roy Choudhury, R. B. Thapa, Y. Sahoo, T. Ohulchanskyy, A. N. Cartwright, K.-S. Lee, P. N. Prasad, *Adv. Mater.* **2007**, *19*, 232.
- [5] D. V. Talapin, C. B. Murray, *Science* **2005**, *310*, 86.
- [6] J. M. Luther, M. Law, Q. Song, C. L. Perkins, M. C. Beard, A. J. Nozik, *ACS Nano* **2008**, *2*, 271.
- [7] G. Konstantatos, J. Clifford, L. Levina, E. H. Sargent, *Nat. Photonics* **2007**, *1*, 531.
- [8] E. J. D. Klem, D. D. MacNeil, P. W. Cyr, L. Levina, E. H. Sargent, *Appl. Phys. Lett.* **2007**, *90*, 183113.
- [9] X. Zhao, I. Gorelikov, S. Musikhin, S. Cauchi, V. Sukhovatkin, E. H. Sargent, E. Kumacheva, *Langmuir* **2005**, *21*, 1086.
- [10] S. Hinds, S. Myrskog, L. Levina, G. Koleilat, J. Yang, S. O. Kelley, E. H. Sargent, *J. Am. Chem. Soc.* **2007**, *129*, 7218.
- [11] G. Konstantatos, L. Levina, A. Fischer, E. H. Sargent, *Nano Lett.* **2008**, *8*, 1446.
- [12] C. Paquet, F. Yoshino, L. Levina, I. Gourevich, E. H. Sargent, E. Kumacheva, *Adv. Funct. Mater.* **2006**, *16*, 1892.